Mineralium Deposita
https://doi.org/10.1007/s00126-018-0833-1

ARTICLE

In situ Pb-Pb isotopic dating of sulfides from hydrothermal deposits: a case study of the Lala Fe-Cu deposit, SW China

Wei Terry Chen[1,2] · Mei-Fu Zhou[1,2] · Xiaochun Li[2] · Jian-Feng Gao[1] · Zhian Bao[3] · Honglin Yuan[3]

Received: 7 August 2017 / Accepted: 3 August 2018

Abstract

Precisely dating different generations of mineralization is important for understanding the origin and tectonic environment of ore formation. In this study, we have dated two generations of sulfides from the Lala Fe-Cu deposit, SW China, using in situ Pb-Pb isotopic data obtained by the LA-MC-ICPMS technique. The Lala deposit is composed of Fe-Cu ore bodies hosted in sedimentary-volcanic rocks of the Paleoproterozoic Hekou Group. It has a paragenetic sequence of pre-ore banded pyrite (Stage I) and Na alteration (Stage II), followed by early Fe (Stage III) and late Cu (Stage IV) mineralization. The sulfides in the deposit have dominantly formed in two stages, including pyrite from stratiform pyrite bands in the host rocks (i.e., Stage I) and epigenetic pyrite-chalcopyrite in Fe-Cu ore (i.e., Stage IV). The sulfides of both stages have highly radiogenic Pb isotopic ratios which form linear trends in the $^{207}Pb/^{204}Pb$ versus $^{206}Pb/^{204}Pb$ diagram. The regression trend for Stage I pyrite grains defines an errorchron age of 1669 ± 110 Ma (MSWD = 32), undistinguishable from zircon LA-ICPMS U-Pb ages of volcanic rocks in the Hekou Group (i.e., ~ 1700 Ma). The regressions for Stage IV pyrite and chalcopyrite yield younger errorchron ages of 1088 ± 88 Ma (MSWD = 93) and 1053 ± 220 Ma (MSWD = 15), respectively. Taking pyrite and chalcopyrite together, an errorchron age of 1053 ± 75 Ma (MSWD = 108) is obtained. These errorchron ages agree well with the molybdenite Re-Os age of the Fe-Cu ore (1086 ± 8 Ma). Despite the large error and MSWD values that are interpreted to be related to the small variation of initial ratios, or post-ore open system behavior, the good agreement with the precise zircon U-Pb and molybdenite Re-Os ages indicates that the Pb-Pb errorchron ages for Stage I and IV sulfides are geologically meaningful. Therefore, this study shows that the in situ Pb isotopic analyses can yield geologically meaningful Pb-Pb ages for radiogenic Pb-rich sulfide minerals. We also propose that in situ Pb-Pb isotopic dating may be more promising for Precambrian deposits containing sulfides with ingrown Pb, particularly for those involving multiple mineralization/hydrothermal events but without relevant minerals for precise Re-Os or U-Pb dating.

Keywords Sulfides · fs-LA-MC-ICPMS · In situ Pb isotopic analyze · Pb-Pb errorchron age · Lala deposit

Editorial handling: D. Huston

Electronic supplementary material The online version of this article (https://doi.org/10.1007/s00126-018-0833-1) contains supplementary material, which is available to authorized users.

✉ Wei Terry Chen
chenwei@mail.gyig.ac.cn

[1] State Key Laboratory of Ore Deposit Geochemistry, Institute of Geochemistry, Chinese Academy of Sciences, Guiyang 550002, China

[2] Department of Earth Sciences, University of Hong Kong, Pokfulam Road, Hong Kong, China

[3] State Key Laboratory of Continental Dynamics, Department of Geology, Northwest University, Xi'an 710069, China

Introduction

Formation of hydrothermal deposits commonly involves multiple mineralization/alteration events which may have age intervals of tens to hundreds of million years (Weihed et al. 2005; Zhou et al. 2014). Precisely dating each generation of mineralization/alteration is important for understanding the ore-forming processes and tectonic environments. However, for many deposits, such age constraints are difficult to achieve owing to the lack of suitable phases for dating (such as molybdenite Re-Os, monazite or titanite U-Th-Pb) that can be unequivocally linked to each generation of mineralization, particularly for those deposits that have experienced post-ore modification. Pyrite and chalcopyrite are common constituents in a wide variety of hydro-

Published online: 18 August 2018

thermal ore deposits and are commonly associated with multiple generations of mineralization/alteration. Thus, dating these sulfide minerals from multiple hydrothermal stages is potentially useful for constraining the timing and origin of multiple mineralization/hydrothermal events. Traditionally, Re-Os, Rb-Sr, and Pb-Pb isotopes of sulfide separates have been used to date various types of hydrothermal or orthomagmatic deposits (Frei and Kamber 1995; Stein et al. 2001; Yang and Zhou 2001; Huang et al. 2013; Zhao et al. 2013). However, these dating methods are generally dissolution-based, and thus, it is difficult to obtain ages for multiple mineralization/alteration events because specimens or individual sulfide grains can involve multiple stages of formation. For example, pyrite commonly displays complex growth textures (Large et al. 2009).

In recent years, laser ablation multiple-collector inductively coupled plasma mass spectrometry (LA-MC-ICPMS) has been proved to be a useful instrument for rapid, inexpensive in situ Pb isotopic analyses of sulfides (Meffre et al. 2008; Souders and Sylvester 2010; Darling et al. 2012; Yuan et al. 2013; Potra and Macfarlane 2014). This technique has the capability of revealing grain- or subgrain-scale isotopic variations at a high-spatial resolution (< 30 μm in diameter and < 10 μm in depth) and is able to precisely obtain Pb isotopic compositions of different generations of sulfides at the thin-section scale. Indeed, the feasibility of dating sulfides by the LA-MC-ICPMS Pb-Pb isochron method has been successfully applied to orthomagmatic deposits (Darling et al. 2012), but such a method has yet to be applied to hydrothermal deposits.

In this study, we obtained femtosecond LA-MC-ICPMS (fs-LA-MC-ICPMS) Pb isotopic data for the sulfides from the Lala Fe-Cu deposit, SW China, to test the utility of in situ sulfide Pb-Pb isotopic dating on hydrothermal ore deposits. This deposit contains abundant pyrite and chalcopyrite that formed during several generations (Zhou et al. 2008; Chen and Zhou 2012). Recent molybdenite Re-Os and allanite U-Pb age results show that sulfides of the Fe-Cu ore have mainly formed at ~ 1080 Ma, and were modified by Neoproterozoic hydrothermal events between ~ 850 and ~ 780 Ma (Chen and Zhou 2012, 2014; Zhou et al. 2014; Zhu et al. 2018). There are also "stratiform" pyrite bands that are locally interlayered in the ore-hosting, Paleoproterozoic (~ 1700 Ma) Hekou Group, but these bands were thought to be either syngenetic in origin (Chen et al. 1992; Chen and Xia 2001) or genetically related to the epigenetic Fe-Cu mineralization (Zhu 2011; Chen and Zhou 2012). In this contribution, we described the mineralogical characteristics of multiple-stage sulfides and conducted in situ LA-MC-ICPMS Pb isotopic analyses on sulfides from both the Fe-Cu ore and "stratiform" pyrite bands. The new dataset allows us to calculate Pb-Pb ages for these sulfides and to testify the reliability of these ages by comparing them with previously obtained Re-Os and U-Th-Pb ages.

Geological background

Regional geology

The Yangtze Block is bounded by the Cathaysia Block to the southeast, the Indochina Block to the southwest, the Tibetan Plateau to the west, and the Qinling-Dabie Orogenic Belt to the north (Fig. 1a). In the southwestern Yangtze Block, Proterozoic volcanic-sedimentary sequences include the late Paleoproterozoic Hekou, Dahongshan and Dongchuan groups (~ 1700 Ma; Chen et al. 2013a; Greentree and Li 2008; Zhao et al. 2010), and the Meso- to Neoproterozoic Huili, Kunyang, and Julin groups (~ 1100–900 Ma; Chen and Chen 1987; Chen et al. 2014; Geng et al. 2007; Greentree et al. 2006; Sun et al. 2009). The Paleoproterozoic sequences were metamorphosed under upper greenschist-lower amphibolite facies conditions (Li et al. 1988), whereas the Meso- to Neoproterozoic sequences underwent lower greenschist facies metamorphism (Chen and Chen 1987; Li et al. 1988). The Proterozoic strata are intruded by ~ 1050 to ~ 1100 Ma gabbroic and granitic intrusions (Geng et al. 2007; Greentree et al. 2006; Wang et al. 2012) and ~ 740 to ~ 860 Ma granitic, dioritic, and gabbroic intrusions (e.g., Zhou et al. 2002, 2006; Li et al. 2003a). These Mesoproterozoic plutons have the geochemical affinities to intra-plate magmatism, and are thought to have formed in a continental rift setting (Chen et al. 2014; Zhu et al. 2016), whereas the Neoproterozoic plutons have been interpreted as either arc-related (Zhou et al. 2002, 2006) or mantle plume-related (Li et al. 2003a).

Numerous Fe-Cu deposits in the southwestern Yangtze Block define the Kangdian Fe-Cu metallogenic province (Fig. 1b) (Sun et al. 1991; Zhao and Zhou 2011). Several large Fe-Cu deposits are present, including, from north to south, the Lala, Xikuangshan, Yinachang, E'touchang, Dahongshan, and Sin Quyen deposits (Sun et al. 1991; Zhao and Zhou 2011; Chen and Zhou 2012; Zhao et al. 2013; Hou et al. 2015; Li et al. 2015; Li and Zhou 2018). These deposits are broadly similar in terms of mineralization style (Ruan et al. 1991; Zhao and Zhou 2011), and the ore bodies are unexceptionally hosted in the Paleoproterozoic sequences (Fig. 1b). The Fe-Cu ores in these deposits contain abundant hematite and magnetite with variable amounts of Cu-Fe-Mo sulfides. Some deposits also show enrichments in Co, U,

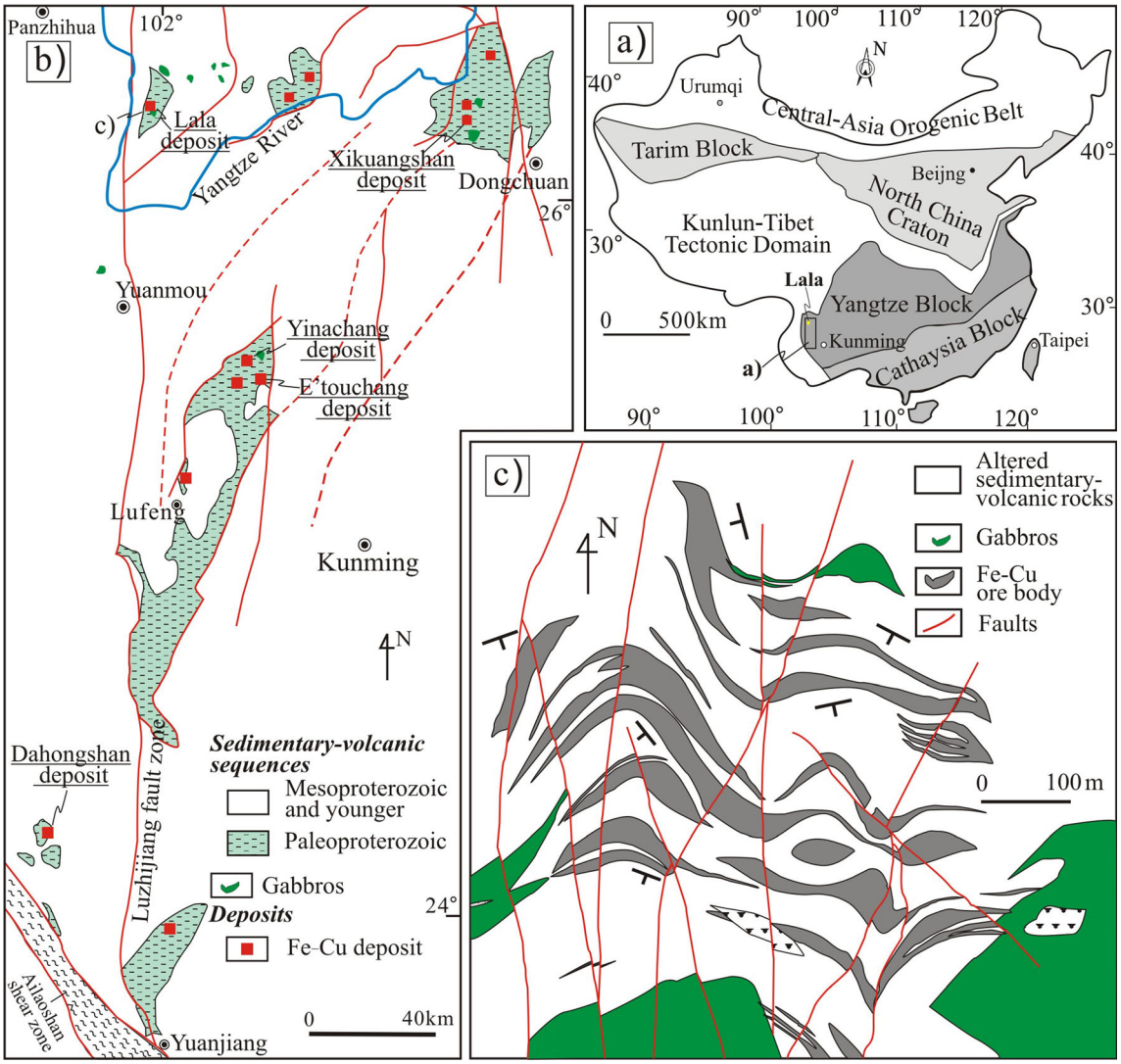

Fig. 1 **a** Tectonic framework of China. **b** Regional geological map of the Kangdian Fe-Cu metallogenic province showing distribution of Fe-Cu deposits (after Wu et al. 1990). **c** A simplified geological map of the Luodang open pit of the Lala deposit (at 2036 m level) (after Chen and Zhou 2012)

REE, and F, and thus were classified as iron-oxide copper gold (IOCG) type (Li et al. 2002; Zhao and Zhou 2011; Chen and Zhou 2012).

Geology of the Lala Fe-Cu deposit

The Lala deposit is one of the largest Fe-Cu deposits in the Kangdian metallogenic province and contains more than 200 Mt of ore with an average grade of 13 wt% Fe, 0.92 wt% Cu, 0.018 wt% Mo, 0.022 wt% Co, 0.25 wt% REE_2O_3, and 0.16 ppm Au (Zhu 2011; Chen and Zhou 2012). The ore bodies are lenticular and predominantly strata-bound with thicknesses from several to tens of meters (Fig. 1c). The ore bodies are hosted in albitite, marble, dolostone, mica-schist, and quartzite of the Paleoproterozoic Hekou Group. Both ore and host rocks are foliated and metamorphosed under upper greenschist- to lower amphibolite-facies conditions. The ore bodies are spatially associated with numerous gabbroic plutons of dominantly ~ 1060 and ~ 1700 Ma (Fig. 1c) (Chen et al. 2013a; Zhu 2011). These intrusions have mostly undergone Na alteration, and several Fe ore bodies are distributed along the contacts between the host strata and ~ 1060 Ma intrusions (He 1980).

The Fe-Cu ores are generally massive, banded, and disseminated (Fig. 2), with minor ore present as veins and stockworks. The detailed paragenetic sequence of the deposit has been presented previously (Zhu 2011; Chen and Zhou

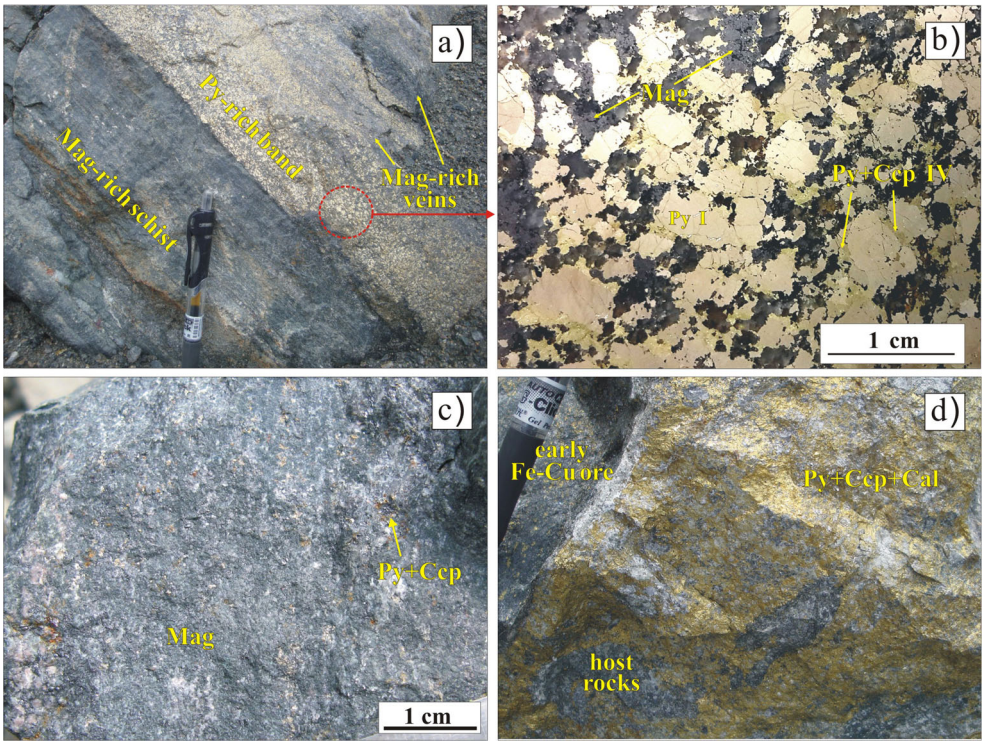

Fig. 2 Macro- and micro-textures of various ores from the Lala deposit. **a** Early Stage I pyrite-rich stratiform bands crosscut or overprint by Mt-rich veins. **b** Stage I pyrite in early bands replaced by late Stage III magnetite, and Stage IV pyrite and chalcopyrite. **c** Early Stage III magnetite ores replaced by Stage IV sulfides. **d** Late unfoliated Stage V pyrite-chalcopyrite veins crosscutting early Fe-Cu ores and host rocks. Mineral abbreviations (after Whitney and Evans 2010): Ccp chalcopyrite; Py pyrite; Mag magnetite

2012; Song 2014), and five stages of alteration and mineralization have been recognized: (I) strata-bound pyrite bands or lenses (Fig. 2a, b) composed dominantly of pyrite with variable amounts of pyrrhotite, quartz, and calcite; (II) pre-ore albite alteration stage in which albite and/or scapolite pervasively overprint the host rocks; (III) an Fe stage dominated by magnetite, albite, and apatite; (IV) the main Cu stage comprising mainly pyrite, pyrrhotite, chalcopyrite, calcite, and micas intergrown with variable amounts of molybdenite, REE minerals, quartz, and apatite; and (V) unfoliated veins of chalcopyrite ± pyrite (Fig. 2d). Stages I to IV are foliated and metamorphosed.

Paragenetic sequence of sulfides

Mineralogical observations of sulfides from the Lala deposit were conducted with a JEOL JXA8100 electron microprobe at the Guangzhou Institute of Geochemistry, Chinese Academy of Sciences, Guangzhou, China. The BSE images are used to characterize the morphology and internal textures of different generations of pyrite and chalcopyrite and their textural relationships with other hydrothermal minerals. Two major generations of pyrite and/or chalcopyrite are identified and examined throughout the Lala deposit, including Stage I "stratiform" pyrite bands and Stage IV pyrite-chalcopyrite.

Stage I pyrite

Irregular aggregates of densely clustered, medium- to coarse-grained, anhedral to subhedral pyrite grains (with minor pyrrhotite) are concentrated as "stratiform" bands or discrete ellipsoids in the host rocks (Fig. 2a) and were considered to be syngenetic in origin as these sulfides do not show clear replacement textures with host rock minerals (Chen and Xia 2001). There are also a few isolated, subhedral to euhedral pyrite crystals distributed along bedding planes (Fig. 3b). In some samples, these pyrite grains are variably recrystallized or folded and locally contain pores or inclusions of fine-grained minerals that form the host rocks (Fig. 3a).

Stage IV pyrite and chalcopyrite

Both pyrite and chalcopyrite are the dominant sulfides in Stage IV Cu mineralization. In the places where Stage I "stratiform" pyrite bands are overprinted by Stage IV Cu mineralization, the pyrite grains generally exhibit complex core-rim textures (Fig. 3a, c–f). For example, under the high-resolution BSE images, it is shown that early, relatively dark Stage I pyrite cores are overgrown by bright, Stage IV pyrite rims (Fig. 3c, e, f). These rims commonly exhibit oscillatory zoning (Fig. 3c, e) and commonly contain abundant anhedral mineral inclusions of chalcopyrite,

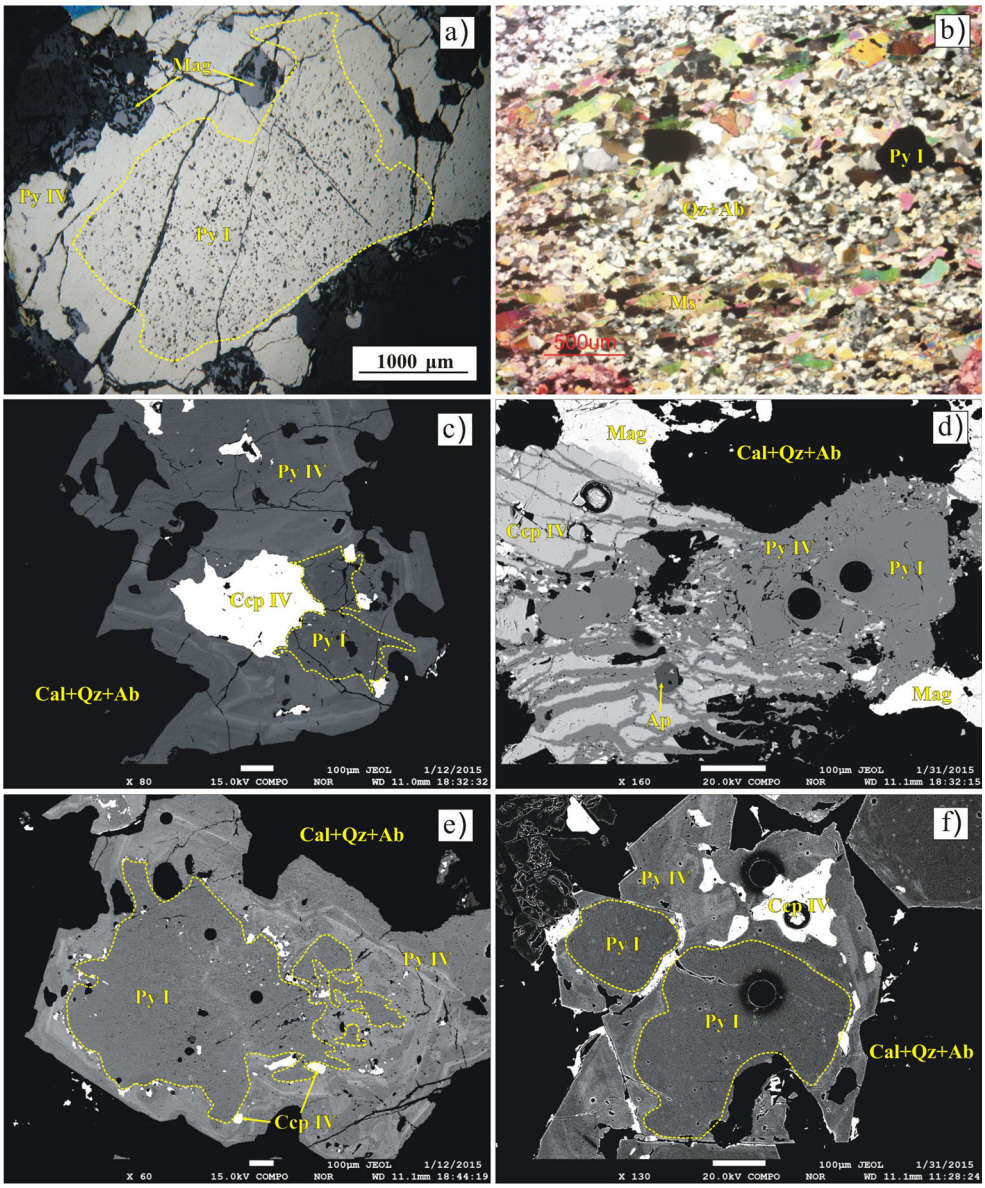

Fig. 3 Photomicrographs of different generations of sulfides from the Lala deposit. **a** Early, Stage I pyrite grains replaced by euhedral magnetite and late, Stage IV pyrite. Stage I pyrite core contains abundant inclusions of silicate minerals. **b** Pyrite-bearing schist composed dominantly of quartz, albite, and muscovite with disseminated pyrite. **c** Early, Stage I pyrite core replaced by Stage IV pyrite and chalcopyrite. **d** Stage I pyrite grains replaced by Stage III magnetite and apatite, and Stage IV chalcopyrite and pyrite. **e** Stage I pyrite core overgrown by Stage IV pyrite rims where chalcopyrite inclusions are present. **f** Irregular Stage I pyrite replaced by closely associated pyrite and chalcopyrite of Stage IV. Note that the pyrite rims in **c** and **e** have oscillatory chemical zoning. Mineral abbreviations: Ccp chalcopyrite; Py pyrite; Ap apatite; Mag magnetite; Qz quartz; Ab albite; Cal calcite; Ms muscovite

carbonate, mica, apatite, bastnaesite, and monazite of Stage IV Cu mineralization (Fig. 3c, e, f).

Previous geochronological studies

Fe-Cu mineralization in the Lala deposit was previously considered to be Neoproterozoic, because of biotite Ar-Ar ages of ~ 850 Ma (Greentree 2007) and a Pb-Pb isochron age of 887 Ma for sulfide separates (Sun et al. 2006). This deposit was also inferred to have formed at ~ 1700 Ma (zircon U-Pb ages; Zhou et al. 2011; Wang et al. 2012; Chen et al. 2013a) assuming that it was syngenetic (Chen and Xia 2001). Such an assumption, however, was contradicted by Li et al. (2003b) who reported four molybdenite Re-Os model ages ranging from 928 ± 1 to 1005 ± 1 Ma, but they did not provide detailed description of the samples. Our Re-Os dating of molybdenite from Stage IV Fe-Cu mineralization has yielded a more reliable, weighted average age of 1086 ± 8 Ma (Chen and Zhou 2012), older than previously thought based on the Ar-Ar and Pb-Pb ages. Zhu and Sun (2013), Zhu et al. (2018) have also reported Re-Os ages of ~ 1.3 Ga for chalcopyrite and molybdenite, but these ages do not correlate with tectonothermal events identified in the region

(Zhou et al. 2014). Chen and Zhou (2014) obtained a LA-MC-ICPMS U-Th-Pb age of 1067 ± 41 Ma for primary allanite associated with sulfides, further supporting the molybdenite Re-Os age of 1086 Ma obtained by Chen and Zhou (2012).

Zhou et al. (2014) obtained Ar-Ar ages of biotite in the veins (~ 820 Ma), similar to that obtained by Greentree (2007). This age is undistinguishable from the LA-ICP-MS U-Pb ages of the secondary allanite and Re-Os age of molybdenite in the late, unfoliated veins (~ 850 Ma) (Chen and Zhou 2014; Zhu et al. 2018), representing the timing of post-deformation or remobilization events related to regional subduction during Neoproterozoic (Zhou et al. 2014).

Geochronology of sulfides

Analytical method

In situ lead isotopic analyses of pyrite and chalcopyrite were conducted on 50–100-μm-thick polished sections, using a Nu Plasma™ multi-collector ICP-MS with a femtosecond laser ablation system (NWR UPFemto, ESI, USA) (fs-LA-MC-ICPMS) at the State Key Laboratory of Continental Dynamics, Northwest University, Xi'an, China. Detailed description of the measuring procedures is available in Chen et al. (2013b) and Yuan et al. (2015). Argon and helium were used as the carrier gases for laser ablation. The aerosol from the ablation cell was mixed with Tl (argon with Tl) in a glass aerosol homogenizer and then introduced into the ICP. During the instrumental analysis, the intensities of the ion beams of ^{202}Hg, ^{203}Tl, ^{204}Pb + Hg, ^{205}Tl, ^{206}Pb, ^{207}Pb, and ^{208}Pb were simultaneously monitored with the Faraday collectors L4, L3, L2, L1, Ax, H1, and H2, respectively. High-temperature-activated carbon was used to filter Hg contained in the carrier gases, which significantly reduced the Hg background signal by 48% and lowered the detection limit of the analyses (Yuan et al. 2015). The concentrations of Pb and Hg in the gas blank were lower than 10 and 20 pg/l, respectively, and thus their contributions for the analyses were negligible (Chen et al. 2013b). Thallium was used to correct for instrumental mass discrimination, and ^{202}Hg was used to correct for the isobaric interference of ^{204}Hg on ^{204}Pb. The calculated interference of ^{204}Hg on ^{204}Pb was achieved using the natural abundance ratio ^{204}Hg/^{202}Hg = 0.229883 (^{202}Hg = 0.29863 and ^{204}Hg = 0.06865) adjusted for instrumental mass fractionation as monitored by the ^{205}Tl/^{203}Tl ratio.

The MC-ICP-MS data was acquired by the time-resolved analysis (TRA) mode with an integration time of 0.2 s, and laser ablation was performed in the line scan ablation mode at a speed of 5 μm/s with the laser beam focused on the sample surface. Each line scan analysis consisted of background collection for 40 s followed by an additional 50 s of ablation for signal collection and 40 s of wash time to reduce memory effects and to allow the instrument to stabilize after each analysis. All of the recorded Pb and Hg signals were corrected for background by subtracting the background signals (gas blank and dark noisy signals which are related to detector noise for Faraday systems: e.g., Johnson noise) from the corresponding gross signals (signals obtained after firing the laser), whereas the Tl signals were corrected for background by subtracting the average dark noisy signals (stability < 25 ppm at 10 min). To ensure the stability of ^{208}Pb signal obtained from different samples with disparate Pb concentrations, samples were ablated with laser line scans approximately 120 μm in length and 30–65 μm in width with adjustable laser frequency. NIST SRM 610 was used as a quality control sample (Yuan et al. 2013) and was analyzed once for every five sample points. The obtained values of Pb isotopic compositions of NIST SRM 610 in this study are the following: ^{208}Pb/^{204}Pb = 36.960 ± 0.003; ^{207}Pb/^{204}Pb = 15.507 ± 0.001 to 15.521 ± 0.002; ^{206}Pb/^{204}Pb = 17.043 ± 0.001 to 17.062 ± 0.002 (2σ) (n = 107; Supplementary Table A1), similar to the reference values: ^{208}Pb/^{204}Pb = 36.964 ± 0.022; ^{207}Pb/^{204}Pb = 15.504 ± 0.001; ^{206}Pb/^{204}Pb = 17.045 ± 0.008 (2σ) (Jochum and Stall 2008). In situ Pb isotopic compositions of different generations of sulfides appear in Supplementary Table 1.

Analytical results

Both stages of pyrite and chalcopyrite have a wide range of Pb isotopic ratios (Supplementary Table 1; Figs. 4 and 5). The early, Stage I pyrite grains have a radiogenic Pb isotopic signature with ^{206}Pb/^{204}Pb, ^{207}Pb/^{204}Pb, and ^{208}Pb/^{204}Pb ratios ranging from 16.220 to 23.607, 15.398 to 16.134, and 35.765 to 39.700, respectively (Supplementary Table 1; Fig. 4). In plots of ^{206}Pb/^{204}Pb versus ^{207}Pb/^{204}Pb and ^{206}Pb/^{204}Pb versus ^{208}Pb/^{204}Pb, these analyses define linear trends (Figs. 5a and 6a). The ^{206}Pb/^{204}Pb-^{207}Pb/^{204}Pb correlation, calculated using Isoplot software package (Ludwig 2003), yielded an errorchron age of 1669 ± 110 Ma (Model 2; MSWD = 32) (Fig. 5a).

Pyrite and chalcopyrite of Stage IV have similar Pb isotopic ratios that are much more radiogenic than those of the

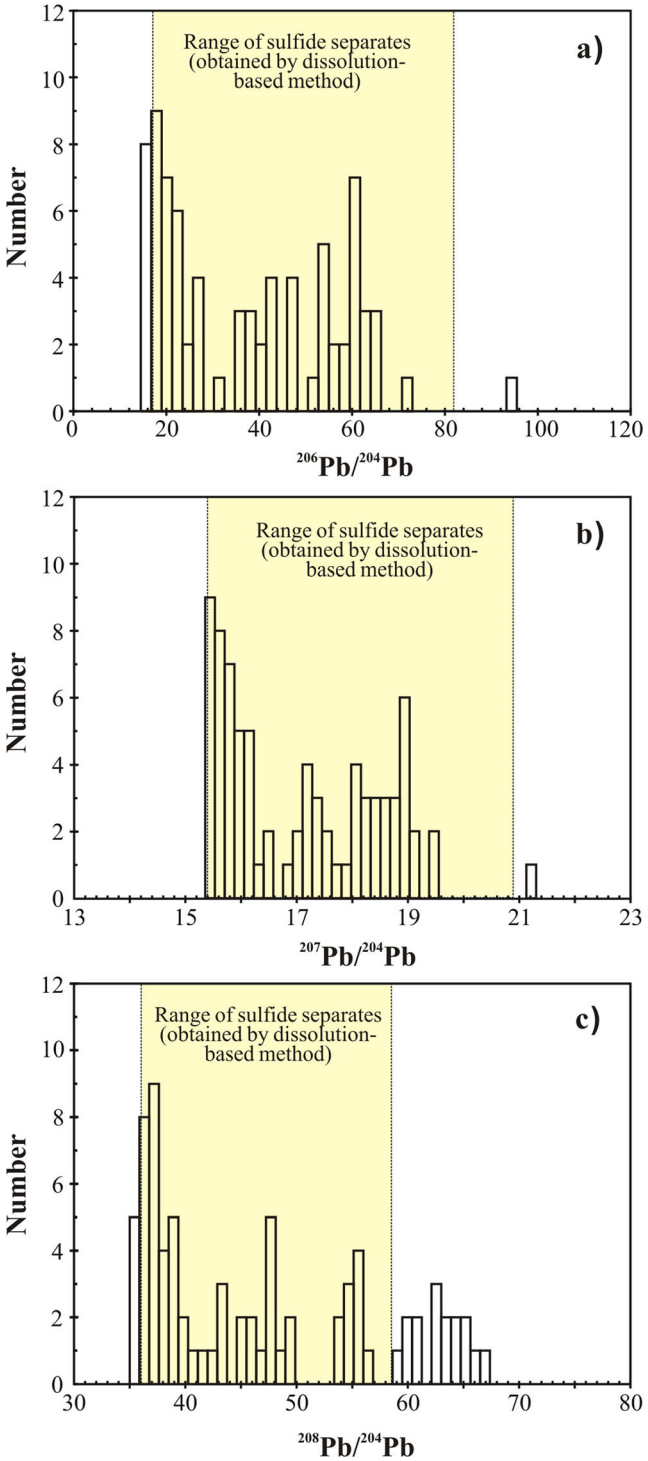

Fig. 4 Comparison of sulfide $^{206}Pb/^{204}Pb$ (**a**), $^{207}Pb/^{204}Pb$ (**b**), and $^{208}Pb/^{204}Pb$ (**c**) isotopic ratios obtained by in situ fs-LA-MC-ICP-MS and dissolution-based methods. The data by dissolution-based method is from Sun et al. (2006) and Huang et al. (2015)

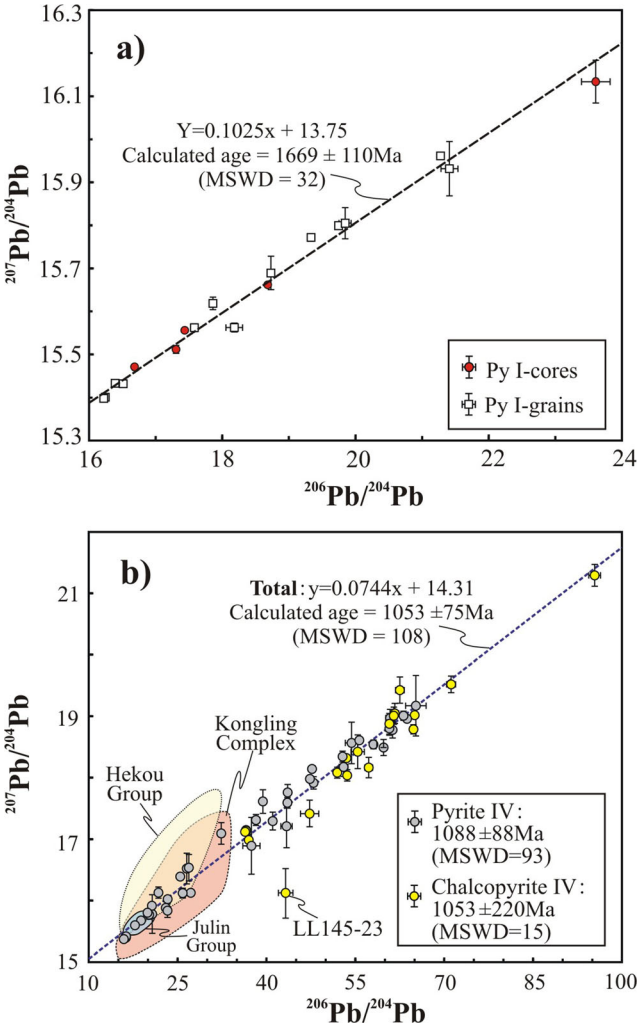

Fig. 5 Plots of $^{206}Pb/^{204}Pb$ versus $^{207}Pb/^{204}Pb$ ratios of Stage I (**a**) and IV (**b**) sulfides from the Lala deposit. Analyses of all stages define linear trends yielding errorchron ages. Also plotted in **b** are the Pb isotopic ratios of rocks from the 1.7 Ga Hekou Group (Huang et al. 2015), Archean Kongling Complex (Zhang 2008), and ~1.05 Ga Julin Group (Deng 2000)

early, Stage I pyrite (Supplementary Table 1; Figs. 5b and 6b). They have broad ranges of $^{206}Pb/^{204}Pb$, $^{207}Pb/^{204}Pb$, and $^{208}Pb/^{204}Pb$ ratios from 15.919 to 95.401, 15.371 to 21.293, and 35.713 to 66.609, respectively. In the $^{206}Pb/^{204}Pb$ versus $^{207}Pb/^{204}Pb$ plot (Fig. 5b), all the analyses define a linear trend. Excluding LL145-23 (Fig. 5b), the remaining analyses in the regression line yield an errorchron age of 1053 ± 75 Ma (Model 2; MSWD = 108). If plotted separately, the regressions defined by the chalcopyrite and pyrite yield undistinguishable errorchron ages of 1053 ± 220 Ma (Model = 2; MSWD = 93) and 1088 ± 88 Ma (Model 2; MSWD = 15), respectively (Fig. 5b). In the $^{206}Pb/^{204}Pb$ versus $^{208}Pb/^{204}Pb$ plot, the sulfides do not yield a linear trend (Fig. 6b).

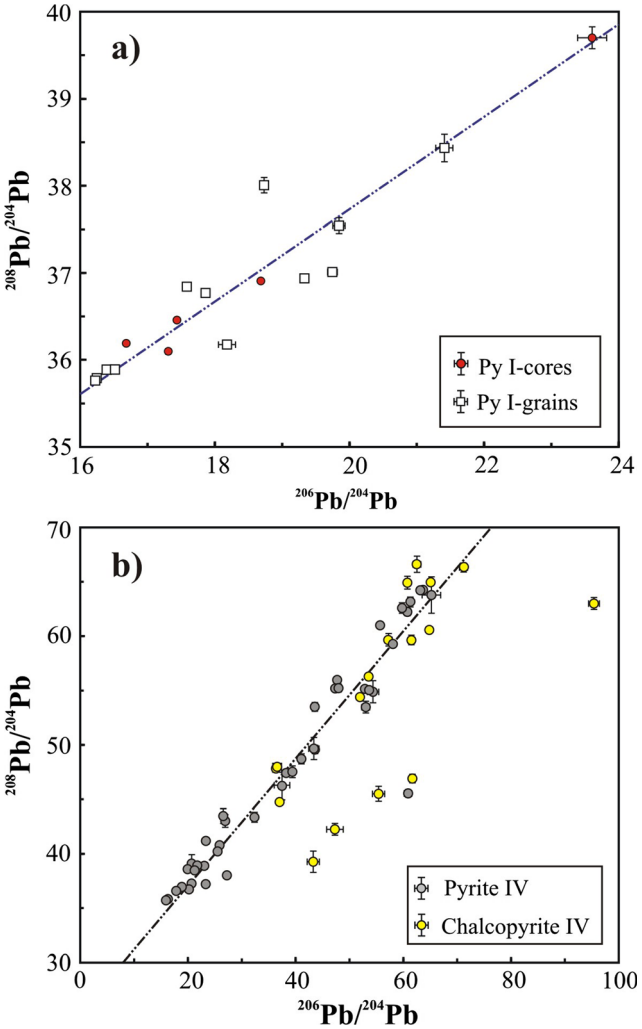

Fig. 6 Plots of $^{206}Pb/^{204}Pb$ versus $^{208}Pb/^{204}Pb$ ratios of Stage I (**a**) and IV (**b**) sulfides from the Lala deposit

Discussion

Reliability of the in situ Pb-Pb errorchron ages

The in situ Pb isotopic ratios of the sulfides are broadly comparable to those previously obtained by dissolution-based measurements for sulfide separates (Fig. 4) (Sun et al. 2006; Huang et al. 2015), suggesting that our in situ Pb isotopic data are reliable. The calculated ages for the two stages of sulfides have high MSWD values (15–108), indicating that the scatter is beyond the assigned analytical uncertainty for the data points. As indicated by Brooks et al. (1972), regression lines with high MSWD values (> 2.5) are called "errorchrons," and their interpretation/geological significances should be treated with caution, unless the geological contexts are well understood. In general, the excess scatter and resultant "errorchron" ages can be produced by (1) mixing of different isotopic sources, (2) variation in the initial ratios and/or initial age of the samples, and/or (3) post-ore open system behavior (Dickin 2005).

The highly radiogenic Pb isotopic ratios and linear trends (Figs. 5 and 6) cannot be explained by mixing of fluids sourced from isotopically different Pb reservoirs, as such reservoirs with highly radiogenic Pb ($^{206}Pb/^{204}Pb$ to 95.401 and $^{207}Pb/^{204}Pb$ to 21.293; Supplementary Table 1) are not known in the region (Fig. 5). Variation of initial age of the samples is also not evident, as the micro- and macro-textural relationships clearly show that each stage of sulfides has formed at the same paragenetic position (Figs. 2 and 3) (Chen and Zhou 2012; Zhu and Sun 2013). Contamination of different generations of sulfides during laser ablation is also unlikely as it was carefully monitored by time-resolved analytical signals during analyses. On the other hand, small variations of initial ratios are likely because several plots do deviate from the regression lines (Fig. 5). In order to quantitatively estimate variation of initial ratios, we calculated initial $^{207}Pb/^{204}Pb$ ratios by projecting analyses along the errorchron corresponding to the crystallization age (i.e., ~ 1050 Ma), on the basis of an assumed initial value of $^{206}Pb/^{204}Pb$ (Darling et al. 2012). We used the lowest measured ratio of 15.919 as the assumed initial $^{206}Pb/^{204}Pb$ value (Fig. 5b) and calculated the initial $^{207}Pb/^{204}Pb_i$ values for the sulfides of the Fe-Cu mineralization to range from 15.087 to 15.959 (Fig. 7), consistent with a variation of the initial ratios. However, it is important to note that the calculated values show a significant peak at ~ 15.470 (Fig. 7), supporting that most of the analyzed sulfides precipitated from fluids with a common initial ratio.

Post-ore open system behavior is likely for the sulfides of both stages, because some of the sulfides were variably recrystallized during late metamorphism or deformation (Chen and Zhou 2012). Greenschist or higher-grade metamorphism are able to "clean" inclusions and trace element budgets in the primary pyrite, and the resultant pyrite would be relatively "pure" in terms of trace element contents (Craig and Vokes 1993). Thus, the primary ratios can be variably modified, possibly resulting in the scattering and high MSWD values of our samples (Fig. 5). However, the Pb-Pb errorchron ages of both stages agree within uncertainty with the zircon LA-ICPMS U-Pb ages of the felsic volcanic layers in the Hekou Group (1670–1700 Ma; Chen et al. 2013a; Zhu et al. 2016) and molybdenite Re-Os and allanite U-Pb ages of the Lala deposit (1086 ± 8 Ma; Chen and Zhou 2012, 2014), respectively,

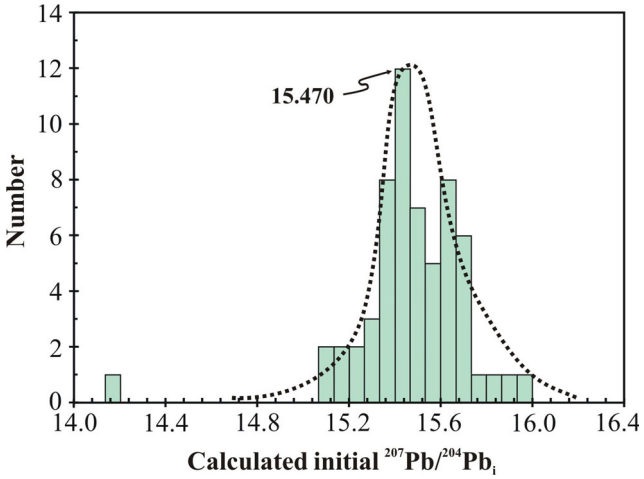

Fig. 7 Histogram of calculated initial $^{207}Pb/^{204}Pb$ ratios of Stage IV Cu mineralizing fluids by assuming an initial $^{206}Pb/^{204}Pb$ ratio. More details are available in the text

implying that the primary Pb-Pb isotopic systems of the two stages of sulfides were largely retained during post-ore tectonothermal or metamorphic overprints at ~ 850 Ma. Therefore, it is concluded that the calculated errorchron ages are geologically meaningful and can be interpreted to represent the timing of early "stratiform" pyrite and sulfides of late Fe-Cu mineralization.

General implications

This study shows that in situ Pb isotopic analyses of sulfides can be useful for unraveling the timing of multiple-stage mineralization in hydrothermal ore deposits. The in situ fs-LA-MC-ICPMS technique with high spatial resolution has the advantage of analyzing hydrothermal sulfides with complex internal textures indicative of multiple hydrothermal/mineralization events. Despite the relatively large errors compared to the molybdenite Re-Os dating or U-Th-Pb dating of U-Th-bearing minerals such as monazite and allanite, the in situ sulfide Pb-Pb errorchron method did provide meaningful constraints on the timing of hydrothermal deposits that may have involved multiple mineralization/alteration events.

This study also demonstrates that detailed paragenetic discrimination of different generations of sulfides and understanding of the potential Pb sources, such as highly radiogenic Pb source, are important for the correct interpretation of the Pb-Pb errorchron ages with high MSWD values. Open system behavior related to deformation or metamorphism may affect the accuracy of the Pb-Pb errorchron ages, but such effects can be reduced, to some extent, by selectively sampling sulfides that are slightly metamorphosed. On the other hand, the effect of potential variation in initial ratios can also be significantly reduced by selecting sulfide targets at a small scale (such as thin-section scale). Our results do show that even at the specimen scale, the sulfides of each stage have highly variable Pb isotopic ratios (e.g., Stage I pyrite of sample LL-132 and Stage IV pyrite of sample LL-53), which are able to produce regression lines defining errorchron ages with smaller MSWDs (Fig. 8).

This study also confirms that radiogenic Pb-rich sulfide minerals are good candidates for in situ Pb-Pb dating. In general, both Th and U are generally incompatible in sulfide structures relative to Pb, and thus, their contents are commonly low (down to < 1 ppm; Darling et al. 2012). In

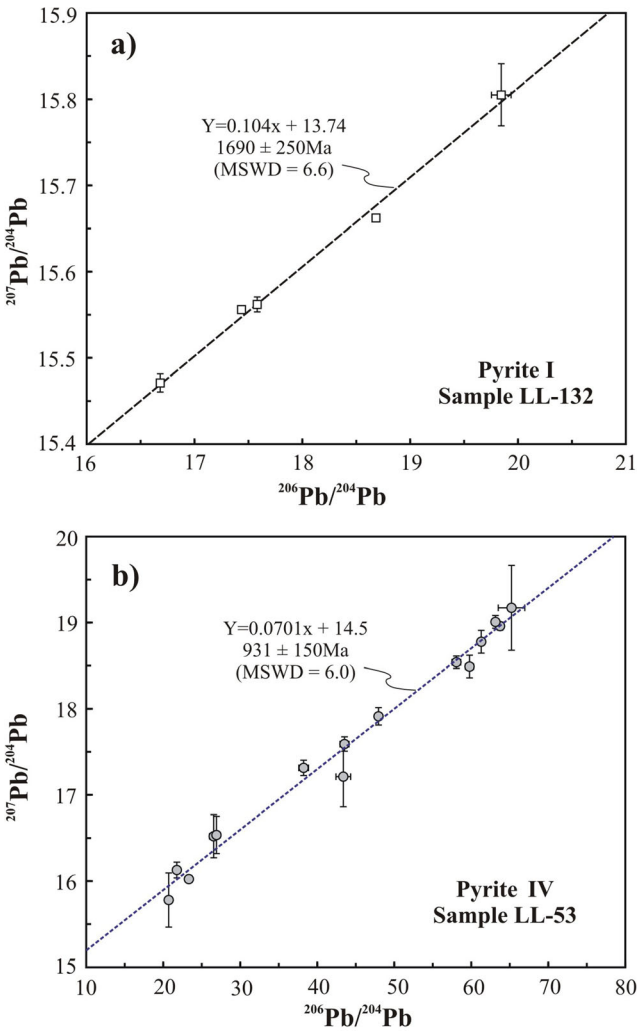

Fig. 8 Plots of $^{206}Pb/^{204}Pb$ versus $^{207}Pb/^{204}Pb$ ratios of Stage I (sample LL-132) (**a**) and Stage IV pyrite (sample LL-53) (**b**). Note that even at a thin-section scale, the pyrite grains have variable Pb isotopic ratios that form regression lines defining meaningful errorchron ages

such cases, the radiogenic Pb decayed from Th or U should be too low to be analyzed with sufficient precision for an accurate Pb-Pb isochron age, particularly for Phanerozoic deposits. In contrast, the sulfides in the Lala deposit are assumed to be enriched in U or Th as the Fe-Cu ores contain abundant U-REE-bearing minerals such as monazite, uraninite, parisite, and bastnasite indicative of REE-U-rich fluids (Li et al. 2002; Chen and Zhou 2012). This assumption is well supported by the unusually high REE contents of the sulfide separates, with total REEs up to 1800 ppm (Zhou et al. 2008). Such high contents of U and REE can be likely related to the fact that the sulfides contain co-precipitated, invisible nanometer-sized particles of U-Th-REE-rich minerals such as monazite or uranitites. However, it is important to note that the presence of U-Th-REE-rich inclusions in the sulfides does not essentially affect the reliability of the errorchron ages, as both the inclusions and hosts are generally precipitated from a common fluid, thus with common initial Pb isotopic ratios. We propose that sulfides from Precambrian hydrothermal deposits, with high U or Th, can be successfully dated by this method.

Conclusions

This study shows that the fs-LA-MC-ICPMS technique is powerful for analyzing Pb isotopic ratios of different stages of sulfide minerals in a single deposit. We also demonstrate that the in situ analyses can yield geologically meaningful Pb-Pb errorchron ages for radiogenic Pb-rich sulfide minerals in the Lala deposit. The Pb isotopic analyses form linear trends defining geologically meaningful errorchron ages of ~1670 Ma for the early syngenetic pyrite and ~1050 Ma for the sulfides in the major Fe-Cu mineralization, respectively. The large errors and MSWD values are likely produced by small variations in the initial ratios, or post-ore open system behavior during late metamorphism or deformation. However, such effects can be avoided by selectively sampling less metamorphosed or deformed sulfides at a small scale. This work signifies that combined textural observations and in situ Pb-Pb isotopic analyses of sulfides are useful for constraining timing of hydrothermal deposits, particularly those of Precambrian ones, the formation of which may have involved multiple alteration/mineralization or overprinting events. Moreover, Precambrian deposits more likely contain sulfides with high contents of radiogenic Pb due to long-term decay of U or Th, and thus are potentially good candidates for in situ Pb-Pb isochron dating.

Acknowledgments We thank Mr. Qiu Wenhong and Liu Zerui during Pb isotopic measurement in Northwest University. Special thanks are due to Prof. Julian Pearce for providing constructive suggestions on an early draft of the manuscript. We are grateful to the official reviews by David Huston and an anonymous reviewer, and editorial handling by Georges Beaudoin.

Funding information This study is supported by the National Key R&D Program of China (2017YFC0602302), Key Research Program of Frontier Sciences, CAS (QYZDB-SSW-DQC008), and the "CAS Hundred Talents" Project to Jian-Feng Gao.

References

Brooks C, Hart SR, Wendt I (1972) Realistic use of two-error regression treatments as applied to rubidium-strontium data. Rev Geophys 10(2):551–577

Chen WT, Sun WH, Wang W, Zhao JH, Zhou MF (2014) "Grenvillian" intra-plate mafic magmatism in the southwestern Yangtze Block, SW China. Precambrian Res 242:138–153

Chen WT, Zhou MF (2012) Paragenesis, stable isotopes, and molybdenite Re-Os isotope age of the Lala iron-copper deposit, Southwest China. Econ Geol 107:459–480

Chen WT, Zhou MF, Zhao XF (2013a) Late Paleoproterozoic sedimentary and mafic rocks in the Hekou area, SW China: implication for the reconstruction of the Yangtze Block in Columbia. Precambrian Res 231:61–77

Chen WT, Zhou MF (2014) Ages and compositions of primary and secondary allanite from the Lala Fe-Cu deposit, SW China: implications for multiple episodes of hydrothermal events. Contrib Mineral Petrol 168:1043–1062

Chen ZL, Chen SY (1987) On the tectonic evolution of the west margin of the Yangzi Block, vol 172. Chongqing Publishing House, Chongqing (in Chinese with English abstract)

Chen GW, Xia B (2001) Study on the genesis of the Lala copper deposit, Sichuan Province: Bulletin of Mineralogy, Petrology and Geochemistry 20:42–44. (in Chinese with English abstract)

Chen GW, Cheng DY, Yu XW (1992) The typomorphic feature of pyrite in the copper deposit of Lala, Sichuan Province. Mineral Petrol 12: 85–91 (in Chinese with English abstract)

Chen KY, Yuan HL, Bao ZA, Zong CL, Dai MN (2013b) Precise and accurate in-situ determination of lead isotope ratios in NIST, USGS, MPI-DING and CGSG glass reference materials using femtosecond laser ablation MC-ICM-MS. Geostand Geoanal Res 38:5–21

Craig JR, Vokes FM (1993) The metamorphism of pyrite and pyritic ores: an overview. Mineral Mag 57:3–18

Darling JR, Storey CD, Hawkesworth CJ, Linghtfoot PC (2012) In-situ Pb isotope analysis of Fe-Ni-Cu sulphides by laser ablation multi-collector ICPMS: new insights into ore formation in the Sudbury impact melt sheet. Geochim Cosmochim Acta 99:1–17

Deng SX (2000) The evolution of metamorphism and geochemistry for the Cangshan and Julin Groups in Central Yunnan, China. Unpublished Ph.D thesis, Guangzhou Institute of Geochemistry, Chinese Academy of Sciences. (in Chinese with English abstract)

Dickin AP (2005) Radiogenic isotope geology. Cambridge University Press, Cambridge, UK

Frei R, Kamber BS (1995) Single mineral Pb-Pb dating. Earth Planet Sci Lett 129:261–268

Geng Y, Yang C, Du L, Wang X, Ren L, Zhou X (2007) Chronology and tectonic environment of the Tianbaoshan Formation: new evidence from zircon SHRIMP U-Pb age and geochemistry. Geological Review 53:556–563 (in Chinese with English abstract)

Greentree MR (2007) Tectonostratigraphic analysis of the Proterozoic Kangdian iron oxide-copper province, South-west China. Unpublished PhD thesis, The University of Western Australia

Greentree MR, Li ZX (2008) The oldest known rocks in south-western China: SHRIMP U-Pb magmatic crystallization age and detrital provenance analysis of the Paleoproterozoic Dahongshan Group. J Asian Earth Sci 33:289–302

Greentree MR, Li ZX, Li XH, Wu HC (2006) Late Mesoproterozoic to earliest Neoproterozoic basin record of the Sibao orogenesis in western South China and relationship to the assembly of Rodinia. Precambrian Res 151:79–100

He J (1980) The albite metasomatites and their original rocks, Lala, Huili, western Sichuan. Bull. Chengdu Inst. Geol. Min. Res., Chinese Acad. Geol Sci. 1: 60–79 (in Chinese with English abstract)

Hou L, Ding J, Deng J, Peng HJ (2015) Geology, geochronology, and geochemistry of the Yinachang Fe-Cu-Au-REE deposit of the Kangdian region of SW China: evidence for a Paleo-Mesoproterozoic tectono-magmatic event and associated IOCG systems in the western Yangtze Block. J Asian Earth Sci 103:129–149

Huang XW, Zhao XF, Qi L, Zhou MF (2013) Re-Os and S isotopic constraints on the origins of two mineralization events at the Tangdan sedimentary rock-hosted stratiform Cu-deposit, SW China. Chem Geol 347:9–19

Huang CJ, Li ZQ, Wang J (2015) Pb isotopic features of the Lala IOCG ore deposit in the southwestern margin of the Yangtze Block and their significance. Geol Bull China 31(2/3):501–507 (in Chinese with English abstract)

Jochum KP, Stall B (2008) Reference materials for elemental and isotopic analyses by LA-(MC)-ICP-MS: Successes and outstanding needs. In: Sylvester P (ed) Laser ablation ICP-MS in the Earth sciences: Current practices and outstanding issues. Mineralogical Association of Canada, Vancouver, BC, pp 147–168

Large RR, Danyushevsky L, Hollit C, Maslennikov V, Meffre S, Gilbert S, Bull Stuart B, Scott R, Emsbo P, Thomas H, Sing B, Foster J (2009) Gold and trace element zonation in pyrite using a laser imaging technique: implications for the timing of gold in orogenic and Carlin-style sediment-hosted deposits. Econ Geol 104:635–668

Li FH, Tan JM, Shen YL, Yu FX, Zhou GF, Pan XN, Li XZ (1988) The Presinian in the Kangdian area. Chongqing, China, Chongqing Publishing House, 396 p. (in Chinese with English abstract)

Li ZQ, Hu RZ, Wang JZ, Liu JJ, Li CY, Liu YP, Ye L (2002) Lala Fe-oxide-Cu-Au-U-REE ore deposit, Sichuan China: an example of superimposed mineralization. Bull Mineral Petrol Geochem 21: 258–260 (in Chinese with English abstract)

Li ZQ, Wang JZ, Liu JJ, Li CY, Du AD, Liu YP, Ye L (2003b) Re-Os dating of molybdenite from Lala Fe-oxide-Cu-Au-Mo-REE deposit, southwest China: implications for ore genesis. Contributions to Geology and Mineral Resources Research 18:39–42. (in Chinese with English abstract)

Li ZX, Li XH, Kinny PD, Wang J, Zhang S, Zhou H (2003a) Geochronology of Neoproterozoic syn-rift magmatism in the Yangtze Craton, South China and correlations with other continents. Evidence for a mantle superplume that broke up Rodinia. Precambrian Res 122:85–109

Li XC, Zhou MF (2018) The Nature and Origin of Hydrothermal REE Mineralization in the Sin Quyen Deposit, Northwestern Vietnam. Econ Geol 113(3):645–673

Ludwig KR (2003) Isoplot 3.00: a geochronological toolkit for Microsoft Excel. Berkeley Geochronology Center, Berkeley

Meffre S, Large RR, Scott R, Woodhead J, Chang ZS, Gilbert SE, Danyushevsky LV, Maslennikov V, Hergt JM (2008) Age and pyrite Pb-isotopic composition of the giant Sukhoi Log sediment-hosted gold deposit, Russia. Geochim Cosmochim Acta 72:2377–2391

Potra A, Macfarlane AW (2014) Lead isotope studies of the Guerrero composite terrane, west-central Mexico: implications for ore genesis. Mineral Deposita 49:101–117

Ruan H, Hua R, Cox DP (1991) Copper deposition by fluid mixing in deformed strata adjacent to a salt diaper, Dongchuan area, Yunnan Province, China. Econ Geol 86:1539–1545

Song H (2014) Precambrian copper-iron-gold-uranium polymetallic deposits and their regional metallogeny in southwestern margin of Yangtze Block. Unpublished Ph.D thesis, Chengdu University of Technology. (in Chinese with English abstract)

Souders AK, Sylvester PJ (2010) Accuracy and precision of non-matrix-matched calibration for lead isotope ratio measurements of lead-poor minerals by LA-MC-ICPMS. J Anal At Spectrom 25:975–988

Stein HJ, Markey RJ, Morgan JW, Hannah JL, Schersten A (2001) The remarkable Re-Os chronometer in molybdenite: how and why it works. Terra Nova 13:479–486

Sun K, Shen Y, Liu G, Li Z, Pan X (1991) Proterozoic iron-copper deposits in central Yunnan Province. China University of Geoscience Press, Wuhan, p 169 (in Chinese with English abstract)

Sun Y, Shu XL, Xiao YF (2006) Isotopic geochemistry of the Lala copper deposit, Sichuan Province, China and its metallogenetic significance. Geochimica 35:553–559 (in Chinese with English abstract)

Sun WH, Zhou MF, Gao JF, Yang YH, Zhao XF, Zhao JH (2009) Detrital zircon U-Pb geochronological and Lu-Hf isotopic constraints on the Precambrian magmatic and crustal evolution of the western Yangtze Block, SW China. Precambrian Res 172:99–126

Wang Z, Zhou B, Guo Y, Yang B, Liao Z, Wang S (2012) Geochemistry and zircon U-Pb dating of Tangtang granite in the western margin of the Yangtze Platform. Acta Petrol Mineral 31:652–662 (in Chinese with English abstract)

Weihed P, Arndt N, Billström K, Duchesne JC, Eilu P, Martinsson O, Papunen H, Lahtinen R (2005) Precambrian geodynamics and ore formation: the Fennoscandian Shield. Ore Geol Rev 2:273–322

Whitney DL, Evans BW (2010) Abbreviations for names of rock-forming minerals. Am Mineral 95:185–187

Wu MD, Duan JS, Song XL, Chen LZ, Dan YQ (1990) Geology of Kunyang Group in Yunnan. Yunnan Science and Technology Press, Kunming, p 265 (in Chinese)

Yang JH, Zhou XH (2001) Rb-Sr, Sm-Nd, and Pb isotope systematics of pyrite: implications for the age and genesis of lode gold deposits. Geology 29:711–714

Yuan HL, Chen KY, Bao ZA, Zong CL, Dai MN, Fan C, Yin C (2013) Determination of lead isotope compositions of geological samples using femtosecond laser ablation MC-ICPMS. Chin Sci Bull 58: 3914–3921

Yuan HL, Yin C, Liu X, Chen KY, Bao ZA, Zong CL, Dai MN, Lai SC, Wang R, Jiang SY (2015) High precision in-situ Pb isotopic analysis of sulfide minerals by femtosecond laser ablation multi-collector inductively coupled plasma mass spectrometry. Sci China Earth Sci 58:1713–1721

Zhang JL (2008) The Sr-Nd-Pb isotopic geochemistry of Kongling high-grade terrain of the Yangtze craton (South China) and its tectonic implications. Unpublished Ph.D thesis, China University of Geosciences. (in Chinese with English abstract)

Zhao XF, Zhou MF (2011) Fe-Cu deposits in the Kangdian region, SW China: a Proterozoic IOCG (iron-oxide-copper-gold) metallogenic province. Mineral Deposita 46:731–747

Zhao XF, Zhou MF, Li JW, Selby D, Li XH, Qi L (2013) Sulfide Re–Os and Rb–Sr isotopic dating of the Kangdian IOCG metallogenic province, SW China: implications for regional metallogenesis. Econ Geol 108:1489–1498

Zhao XF, Zhou MF, Li JW, Sun M, Gao JF, Sun WH, Yang JH (2010) Late Paleoproterozoic to early Mesoproterozoic Dongchuan Group in Yunnan, SW China: implications for tectonic evolution of the Yangtze Block. Precambrian Res 182:57–69

Zhou MF, Ma Y, Yan DP, Xia X, Zhao JH, Sun M (2006) The Yanbian Terrane (southern Sichuan Province, SW China): a Neoproterozoic arc assemblage in the western margin of the Yangtze Block. Precambrian Res 144:19–38

Zhou MF, Yan DP, Kennedy AK, Li YQ, Ding J (2002) SHRIMP zircon geochronological and geochemical evidence for Neoproterozoic arc-related magmatism along the western margin of the Yangtze Block, South China. Earth Planet Sci Lett 196:51–67

Zhou JY, Zheng RC, Zhu ZM, Chen JB, Shen B, Li XY, Luo LP (2008) Geochemical characteristics of trace elements of pyrite and its implications to the metallogenesis in the Lala copper deposit. J Mineral Petrol 28:64–71 (in Chinese with English abstract)

Zhou JY, Mao JW, Liu FY, Tan HQ, Shen B, Zhu ZM, Chen JB, Luo LP, Zhou X, Wang Y (2011) SHRIMP U-Pb zircon chronology and geochemistry of albitite from the Hekou Group in the western Yangtze Block. J Mineral Petrol 31(3):66–73 (in Chinese with English abstract)

Zhou MF, Zhao XF, Chen WT, Li XC, Wang W, Yan DP, Qiu HN (2014) Proterozoic Fe-Cu metallogeny and supercontinental cycles of the southwestern Yangtze Block, southern China and northern Vietnam. Earth Sci Rev 139:59–82

Zhu ZM (2011) Lala iron oxide copper gold deposit: metallogenic epoch and metal sources. Unpublished thesis, Chengdu University of Technology (in Chinese with English abstract)

Zhu ZM, Sun YL (2013) Direct Re-Os dating of chalcopyrite from the Lala IOCG deposit in the Kangdian copper belt, China. Econ Geol 108:871–882

Zhu ZM, Zeng LX, Zhou JY, Luo LP, Chen JB, Shen B (2009) Lala iron oxide-copper-gold deposit in Sichuan Province: evidence from mineralography. Geol J China Univ 15:485–495 (in Chinese with English abstract)

Zhu ZM, Tan HQ, Liu YD, Li C (2018) Multiple episodes of mineralization revealed by Re-Os molybdenite geochronology in the Lala Fe-Cu deposit, SW China. Mineral Deposita 53:311–322

Zhu WG, Zhong H, Li ZX, Bai ZJ, Yang YJ (2016) SIMS zircon U-Pb ages, geochemistry and Nd-Hf isotopes of ca. 1.0 Ga mafic dykes and volcanic rocks in the Huili area, SW China: origin and tectonic significance. Precambrian Res 273:67–89